Online Event Detection in Synchrophasor Data with Graph Signal Processing

Jie Shi, Brandon Foggo, Xianghao Kong,
Yuanbin Cheng, Nanpeng Yu
University of California Riverside
Riverside, California 92521
Email: nyu@ece.ucr.edu

Koji Yamashita
Michigan Technological University
Houghton, Michigan 49931
Email: kyamashi@mtu.edu

***Abstract*—Online detection of anomalies is crucial to enhancing the reliability and resiliency of power systems. We propose a novel data-driven online event detection algorithm with synchrophasor data using graph signal processing. In addition to being extremely scalable, our proposed algorithm can accurately capture and leverage the spatio-temporal correlations of the streaming PMU data. This paper also develops a general technique to decouple spatial and temporal correlations in multiple time series. Finally, we develop a unique framework to construct a weighted adjacency matrix and graph Laplacian for product graph. Case studies with real-world, large-scale synchrophasor data demonstrate the scalability and accuracy of our proposed event detection algorithm. Compared to the state-of-the-art benchmark, the proposed method not only achieves higher detection accuracy but also yields higher computational efficiency.**

I. Introduction

Timely detection of abnormal power system phenomena caused by factors such as extreme weather and equipment failure can facilitate system operators in taking corrective control actions to restore the system from an insecure or emergency state. Although the wide-spread adoption of phasor measurement units (PMUs) makes it possible to develop data-driven anomaly detection algorithms, it also brings computational challenges to deal with a large amount of streaming PMU data with strong spatio-temporal correlations. The goal of this paper is to develop a data-driven online detection algorithm of events that cause abnormal phenomena (hereafter, it is called the *abnormal event* in this paper), which is not only computationally efficient but also adequately captures the complex spatio-temporal correlations in the PMU data.

The majority of existing literature for online abnormal event detection can be categorized into five groups. The first group of work uses classical signal processing techniques such as wavelet transforms [1], [2] and short-time Fourier transforms [3] to identify large spectral components in high-frequency bands, which are indicative of power system events. The second group of work detects events based on the forecast residuals of PMU measurements [4], [5], [6]. The third group of work uses the observation that spatial correlations between PMUs could encounter significant changes during abnormal events. Event indicators based on correlation coefficient matrix [7], sample covariance matrix [8], and tensor sample covariance matrix [9] are derived. The fourth group of work performs online event detection based on the observation that the low-rank property of PMU data no longer holds when the system transitions from normal to abnormal state [10] and [11]. The last group of work leverages data mining techniques, such as matrix profile, to detect abnormal events [12].

The complex spatio-temporal correlations in streaming PMU data have not been fully exploited by the existing literature. The spatial correlations among different PMUs are ignored in the first and fifth groups of literature [1], [2], [3], [12]. The temporal dependency of the streaming PMU data is not directly modeled in [6], [7], [8], [9]. The spatial and temporal correlations of PMUs are mixed in the mathematical model of [4], [5] and could not be analyzed explicitly. Although a few papers incorporate spatio-temporal correlations into the analysis, their algorithms are computationally expensive. For example, in the online event detection stage, singular value decomposition [10], [11] and convex optimization problem [4] need to be solved. Thus, they do not scale well to large-scale networks with thousands of PMUs.

In this paper, we fill the knowledge gap by developing a scalable online abnormal event detection algorithm based on graph signal processing (GSP). Our proposed algorithm inherits the computational efficiency and remarkable scalability of the GSP approach. Our proposed algorithm rigorously encodes the spatial and temporal correlations of the streaming PMU data in the weighted adjacency matrix and graph Laplacian of the product graph. A data-driven algorithm is developed to construct the graph Laplacian of the product graph based on the decoupled spatial and temporal correlation matrices. In the offline stage, we first fit a vector autoregressive (VAR) model to capture the intrinsic spatio-temporal correlations of the streaming PMU data. Then a convex optimization

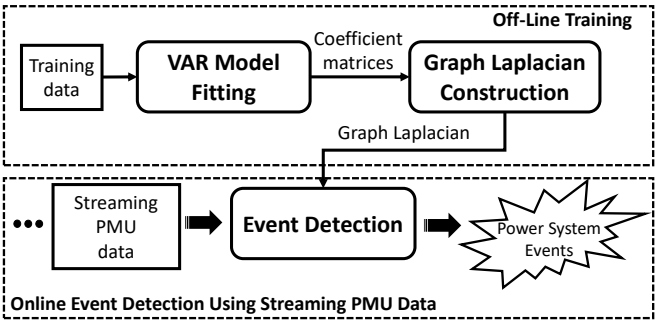

Fig. 1: Overall framework of the proposed abnormal event detection framework based on GSP.

problem is solved online to identify the decoupled spatial and temporal correlations of the PMU data. Our proposed GSP based algorithm has a linear time complexity for online implementation, providing great potential in real-time event detection for very large PMU networks.

The unique contributions of this paper are as follows:

- We develop a computationally efficient and scalable online abnormal event detection algorithm based on GSP for streaming PMU data.
- We propose a novel data-driven approach to construct graph Laplacian of a product graph based on spatial and temporal coefficient matrices.
- We design a general approach to decouple the spatial and temporal correlations in multiple time series based on GSP and vector autoregressive model.

The rest of this paper is organized as follows: Section II first introduces the overall framework of the proposed abnormal event detection algorithm. It then presents the technical methods for estimating spatial and temporal coefficient matrices, constructing graph Laplacian, and detecting abnormal events based on GSP. Section III presents several case studies with real-world PMU data in the United States. The conclusion is stated in Section IV.

II. Abnormal Event Detection Based on Graph Signal Processing

In this section, we first provide an overview of the overall framework of the proposed online abnormal event detection algorithm based on graph inference and graph signal processing. Then we present the key technical methods for modeling spatial-temporal correlations of PMU data, constructing graph Laplacian, and detecting abnormal events with graph signal processing.

A. Overall Framework

The overall framework of the proposed online abnormal event detection algorithm using streaming PMU data is shown in Fig. 1. The proposed abnormal event detection algorithm can be carried out in two stages: off-line training and online abnormal event detection. The off-line training stage contains two key modules: the modeling of spatial-temporal correlations of PMU data and the construction of graph Laplacian. The online event detection stage leverages graph signal processing technique to identify abnormal phenomena in power system operations.

The aim of the off-line training process is to construct a graph Laplacian based on streaming PMU data for the online anomaly detection stage. The constructed graph Laplacian should accurately capture the spatio-temporal correlation among multiple PMUs. The graph Laplacian does not need to be updated frequently since the majority of the underlying transmission network topology and power plants stay the same. In this paper, we construct the graph Laplacian by deriving the spatial and temporal coefficient matrices of the PMU data streams from the vector autoregressive processes. The technical details of the off-line training process will be shown in Section II.B and II.C.

We develop a graph signal processing-based anomaly detection algorithm to detect abnormal power system events in the online stage. The algorithm takes incoming PMU measurements from the phasor data concentrator as inputs and returns the abnormal event indicator before the next data frame arrives. The proposed online anomaly detection procedure is scalable and can be computationally efficient because most of the computational burden takes place in the off-line stage.

B. Inference of Spatial and Temporal Coefficient Matrices for PMU Data Streams

In this subsection, we present a two-step process for inferring spatial and temporal coefficient matrices of multiple PMU time series. In the first step, we model multiple PMU data streams as a vector autoregressive process. In the second step, we derive the spatial and temporal coefficient matrices of the vector autoregressive process. These two coefficient matrices will be used to construct the graph Laplacian in the next subsection.

1) Step I: Model multiple PMU Data Streams as Vector Autoregressive Processes: Suppose we receive streaming data from N PMUs. Let $\boldsymbol{y}_t$ be the data frame of certain measurements recorded by these N PMUs at time stamp t. $\{\boldsymbol{y}_t | t = 1, \cdots, T\}$ is a vector time series. We model the vector time series with the following spatio-temporal model to separate the spatial and temporal correlations:

$$\boldsymbol{y}_t = A\boldsymbol{y}_t + \sum_{j=1}^{p} \Phi_j \boldsymbol{y}_{t-j} + \boldsymbol{\epsilon}_t \tag{1}$$

where A is called the *spatial coefficient matrix*. Φ_j denotes the *j-th temporal coefficient matrix*. $\boldsymbol{\epsilon}_t$ is a white noise vector. p is the order of the model. Note that this spatio-temporal model specification is different from the standard VAR model due to the introduction of spatial coefficient matrix A.

Assuming $(I - A)$ is invertible, we can reformulate (1) into the standard VAR(p) model form:

$$\boldsymbol{y}_t = \sum_{j=1}^{p} (I - A)^{-1} \Phi_j \boldsymbol{y}_{t-j} + (I - A)^{-1} \boldsymbol{\epsilon}_t. \tag{2}$$

Let Ψ_j denote $(I-A)^{-1}\Phi_j$. Ψ_js are the coefficient matrices in the standard VAR(p) model, which can be estimated through multivariate least squares with a training dataset [13]. The model order p can be determined through the Bayesian information criterion (BIC) [14].

2) Step II: Derive Spatial and Temporal Coefficient Matrices: The remaining question is how to find a pair of spatial and temporal coefficient matrices A and Φ_j, that not only satisfies the following constraint but also achieves the highest level of spatio-temporal separation.

$$\Psi_j = (I-A)^{-1}\Phi_j \tag{3}$$

In this study, we focus on solving the first order temporal coefficient matrix, Φ_1, since it captures the majority of the temporal correlations in streaming PMU data. The temporal coefficient matrices with longer time lags can be easily derived once A is known. Furthermore, we only use A and Φ_1 in the graph Laplacian construction. Thus, the temporal coefficient matrix refers to Φ_1 hereafter.

We formulate the following optimization problem to find the spatial and temporal coefficient matrices A and Φ_1:

$$\begin{aligned} \underset{A,\Phi_1}{\text{minimize}} \quad & ||\Phi_1 - I||_F && (4)\\ \text{subject to} \quad & (I-A)\Psi_1 = \Phi_1 && (5)\\ & A = A^T && (6)\\ & \Phi_1 = \Phi_1^T && (7) \end{aligned}$$

where $||\cdot||_F$ denotes the matrix Frobenius norm. The motivation for selecting the objective function (4) is to decouple the spatial and temporal correlations in the most powerful fashion. This can be achieved by suppressing the off-diagonal elements of Φ_1. The resultant Φ_1 primarily captures the temporal correlation while A accounts for the majority of the spatial correlation. While any diagonal matrix could replace the identity matrix in (4), we chose the identity matrix due to its connection to the standard Discrete Fourier Transform (DFT) in graph signal processing. Since graph signal processing-based anomaly detection can be seen as a spatio-temporal generalization of the DFT, it makes sense to keep the temporal component as close to the standard temporal DFT as possible. Constraint (5) is equivalent to (3). Constraints (6) and (7) enforce A and Φ_1 to be symmetric. The reason for enforcing these two constraints will be evident in the graph Laplacian construction process.

Note that the above optimization problem is convex and can be easily tackled by commercial solvers such as Gurobi.

C. Graph Laplacian Construction

In this subsection, we build the graph Laplacian from the spatial and temporal coefficient matrices derived from the VAR model. We first develop a product graph to represent the targeted PMUs' time-series data. Then, we construct the Laplacian matrix for the product graph.

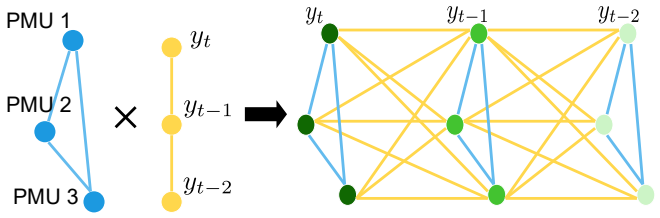

Fig. 2: Product graph construction for PMU data streams.

1) Product Graph: We adopt an undirected product graph to represent the domain of PMU time series $\{\boldsymbol{y}_t, \boldsymbol{y}_{t-1}, \cdots, \boldsymbol{y}_{t-T_w+1}\}$ with a window length of T_w. Formally, the proposed product graph $G = (\mathcal{V}, \mathcal{E})$ is a strong product of a complete graph $G_1 = (\mathcal{V}_1, \mathcal{E}_1)$ and a line graph $G_2 = (\mathcal{V}_2, \mathcal{E}_2)$. The nodes in G_1 and G_2 represent different PMUs and their time stamps. The nodes (also called vertices) and edges of G can be derived from those of G_1 and G_2 [15]:

$$|\mathcal{V}| = |\mathcal{V}_1| \cdot |\mathcal{V}_2| \tag{8}$$

$$\mathcal{E} = \mathcal{E}_1 \otimes \mathcal{E}_2 + \mathcal{E}_1 \otimes I_{|\mathcal{V}_2|} + \mathcal{E}_2 \otimes I_{|\mathcal{V}_1|} \tag{9}$$

where $|\cdot|$ returns the cardinality of a set, $\otimes$ denotes the Kronecker product, and I_N is the identity matrix of size N.

Fig. 2 shows an example of the proposed product graph with three PMUs and a window length $T_w = 3$. In Fig. 2, the blue graph, G_1, on the left has three fully connected nodes and represents the spatial correlations among PMUs. The yellow graph, G_2, in the middle corresponds to the temporal relationship between adjacent time stamps. The resulting product graph is shown on the right hand side.

2) Laplacian Matrix: The Laplacian matrix, L of a graph G can be derived as $L = D - W$, where W is the (symmetric) weighted adjacency matrix. The *degree matrix* D is a diagonal matrix with $D_{mm} = \sum_n W_{mn}$ [16]. The graph Laplacian is symmetric.

To construct the symmetric graph Laplacian matrix representing the PMU data streams, we need to first build the weighted adjacency matrix W of the product graph. We propose to build the weighted adjacency matrix W with the spatial and temporal coefficient matrices A and Φ_1 as follows:

$$W = \begin{bmatrix} A & \Phi_1 & 0 & \cdots & 0 \\ \Phi_1 & A & \Phi_1 & & \vdots \\ 0 & \Phi_1 & \ddots & \ddots & 0 \\ \vdots & & \ddots & A & \Phi_1 \\ 0 & \cdots & 0 & \Phi_1 & A \end{bmatrix} \tag{10}$$

Note that the blue edges of the product graph G in Fig. 2 model the spatial correlations among different PMUs. Thus, the diagonal sub-matrices of W are set as the spatial coefficient matrix A. Similarly, the yellow edges represent the temporal correlations between measurements from two adjacent time stamps in the product graph. Hence, we set the sub-matrices adjacent to the diagonal sub-matrices in W as the temporal coefficient matrix Φ_1. Note that the size of W is $(N \times T_w)$

by $(N \times T_w)$, which means, the size of W depends on the number of PMUs and the window length.

D. Online Abnormal Event Detection

In this subsection, we present the online abnormal event detection algorithm based on graph signal processing. First, we briefly describe the basics of graph signal spectral analysis using graph Fourier transform. Then we explain how to calculate abnormal event indicator for streaming PMU data with graph Fourier transform technique.

1) Graph Fourier Transform: Let $\boldsymbol{s} = [s(1), \cdots, s(n)]$ denote the graph signals at a particular time stamp, where $s(n)$ represents the value of the signal at the n-th node. In this study, $n = N \times T_w$. The graph Fourier transform (GFT) of a signal $\boldsymbol{S}$ converts the original signal $\boldsymbol{s}$ into the Laplacian spectral domain as follows [17]:

$$\boldsymbol{S} = U^{-1}\boldsymbol{s} \tag{11}$$

where $U = [\boldsymbol{u}_1, \cdots, \boldsymbol{u}_n]$ is a matrix of eigenvectors of the graph Laplacian L, i.e., $U\Lambda U^{-1} = L$. Λ is a diagonal matrix consisting of the eigenvalues of L. The graph Laplacian matrix is positive semi-definite by definition. Its eigenvalues are real and non-negative, and its eigenvectors form an orthonormal basis. We follow the convention that the eigenvectors in U are written in an ascending order with respect to their corresponding eigenvalues. It is worth noting that the eigenvectors with smaller eigenvalues correspond to the lower frequency components [16].

2) Abnormal Event Detection in the Laplacian Spectral Domain: The measurements from different PMUs have strong spatio-temporal correlations under the same system configuration. The measurements of an individual PMU vary slowly across time during normal system operations. As a consequence, synchrophasor data under normal operating conditions exhibit low rank property [10], [11].

This low-rank property indicates that the DC component becomes dominant in the Laplacian spectral domain for PMU data under normal operating conditions. When abnormal events occur, the non-DC components, especially the high-frequency ones, become pronounced. Thus, we select the following weighted sum of the non-DC Laplacian spectral components as the abnormal measurement indicator (AMI) for each type of PMU measurement:

$$\text{AMI} = \sum_{i=2}^{n} \lambda_i S(i) \tag{12}$$

where λ_i is the i-th eigenvalue, and $S(i)$ is the coefficient of the i-th Laplacian spectral component. Once a new PMU data frame arrives, the corresponding AMI is calculated.

The voltage and current phasor data gathered from PMUs are typically first converted to into real power P, reactive power Q, voltage magnitude $|V|$, and frequency f for system monitoring and event detection. We call data of this format $PQ|V|f$ data. Note these four types of measurements might not be equally important in detecting different types of abnormal events. To address this issue, we introduce the abnormal

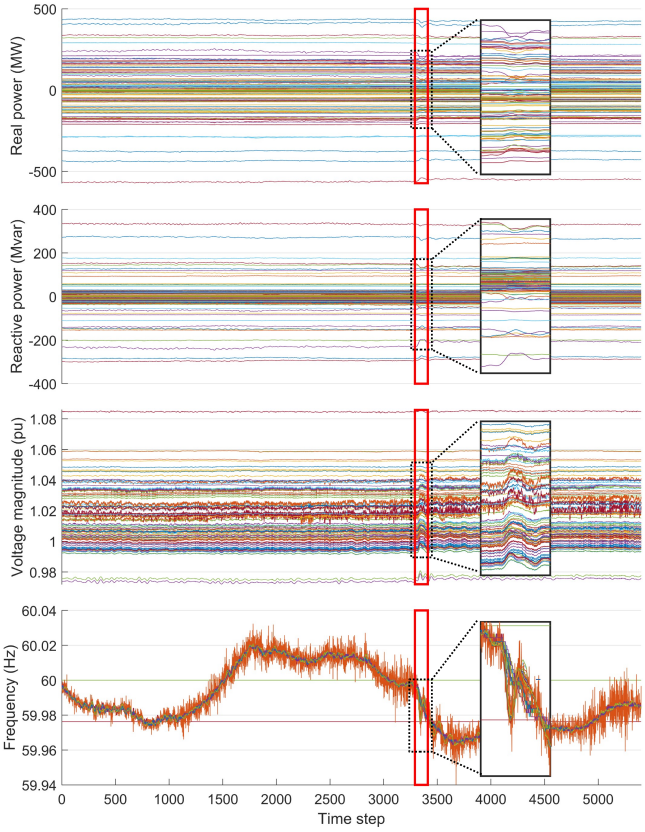

Fig. 3: PQ$|V|$f data of a sample frequency event.

event indicator (AEI), which is a weighted sum of abnormal indicators for PMU measurements of P, Q, $|V|$, and f:

$$\text{AEI} = w_P\text{AMI}_P + w_Q\text{AMI}_Q + w_{|V|}\text{AMI}_{|V|} + w_f\text{AMI}_f \tag{13}$$

where AMI_P, AMI_Q, AMI_V, and AMI_f are the abnormal measurement indicators for P, Q, $|V|$, and f, respectively. w_P, w_Q, $w_{|V|}$, and w_f are the corresponding weights. Once the AEI exceeds a designated threshold, the algorithm reports that an abnormal event is detected.

In this study, we use an adaptive threshold based on moving average:

$$Th(t) = p \cdot \sum_{k=t-1}^{t-K} Th(k) \tag{14}$$

where K is the size of moving window. p is an adjustable parameter.

III. Case Study with Real-World PMU Data

In this section, we evaluate the performance of our proposed abnormal event detection algorithm using synchrophasor data from one of the three interconnections across the U.S. The PMU data is provided by Pacific Northwest National Laboratory (PNNL). The state-of-the-art power system event detection algorithm, OLAP [10], is selected as the benchmark. In this section, we first describe the dataset and the abnormal

TABLE I: Weights of P, Q, $|V|$, and f associated with different categories of events

Weight	w_P	w_Q	$w_{\|V\|}$	w_f
Category 1	0.1	0.3	0.4	0.2
Category 2	0.4	0.3	0.15	0.15
Category 3	0.5	0.3	0.05	0.15

event labeling process. Then, we evaluate the performance of our proposed event detection algorithm based on graph signal processing and the benchmark using different types of real-world events. Finally, we validate the scalability of the proposed algorithm using a Dell workstation with a CPU of Intel Xeon E3-1226 v3 @ 3.30GHz.

A. Data Source, Parameters, and Event Labeling

The historical synchrophasor data corresponding to 30 abnormal power system events in the United States are extracted from the entire dataset. These 30 events fall into three categories: voltage events with faults, voltage events without faults, and frequency events. Each category includes 10 different events. The number of PMUs with valid data during each event period varies between 89 and 138. The sampling rate of PMUs is 30 Hz. 4 minutes of PMU data are used for each event. The actual event occurs in the last three minutes of the 4-minute window. The offline graph Laplacian construction uses the PMU data from the first minute of the 4-minute window. In this study, we first apply z-score normalization on the input $PQ|V|f$ data with a rolling window size of 120 samples, as a preprocessing. The graph window length T_w is set as 2.

The weights associated with abnormal measurement indicators of P, Q, $|V|$, and f are shown in Table I. Based on the domain knowledge, we select different sets of weights to detect different types of power system events. In practice, the event type is often unknown. Thus, abnormal event indicators for different types of events need to be calculated simultaneously to detect all types of events.

The dynamic behavior caused by an event is generally observed in a few seconds. However, the event time stamp provided in the raw dataset is rounded to the minute level. To verify the proposed algorithm and the benchmark, we manually labeled the initiating point of all events up to the second level by inspecting the point-on-wave $PQ|V|f$ data. Figure 3 shows the $PQ|V|f$ data streams of the PMUs for a sample frequency event. The red rectangles indicate the timing when the event occurs.

B. Performance Evaluation for Event Detection Algorithms

In this subsection, we compare the abnormal event detection performance of the proposed approach with that of a benchmark algorithm, OLAP [10], on the 30-event datasets. We follow Algorithm 2 of [10] and the parameters therein. Note that we use $PQ|V|f$ data instead of phasors as OLAP's inputs, which produces four indicators similar to AMI. In this study, we call them AMI_P^O, AMI_Q^O, $\text{AMI}_{|V|}^O$, and AMI_f^O. An

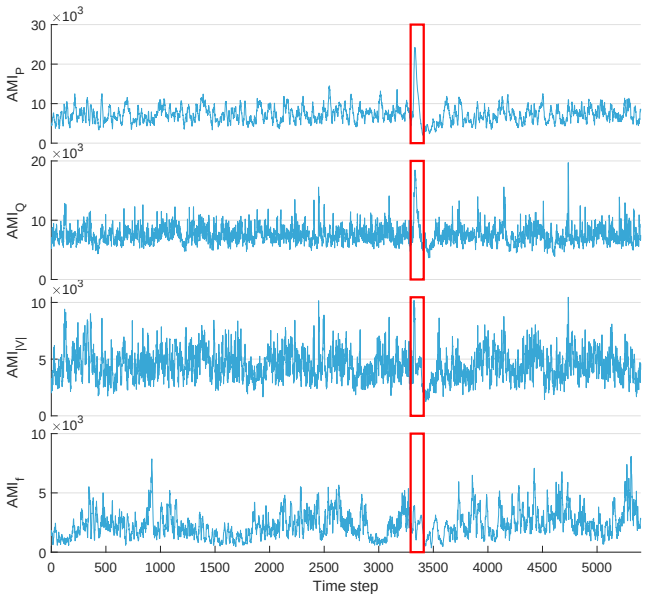

Fig. 4: Abnormal measurement indicators of the proposed GSP based approach for the sample frequency event.

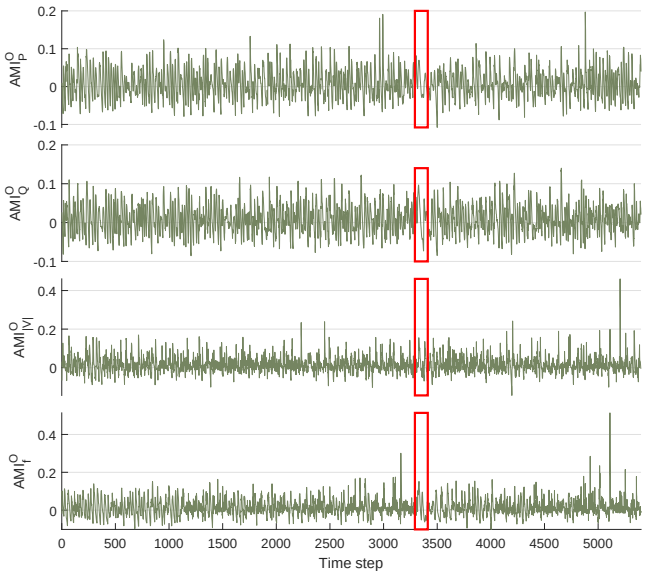

Fig. 5: Abnormal measurement indicators of the OLAP algorithm for the sample frequency event.

abnormal event indicator for OLAP, denoted by AEI^O, is also derived similarly through (13).

We run both algorithms on the last three minutes of $PQ|V|f$ data, which produces two sets of four abnormal measurement indicators for each event. Figures 4 and 5 show the four abnormal measurement indicators provided by the proposed GSP-based approach and the OLAP algorithm for the sample frequency event depicted in Fig. 3. As shown in Figs. 4 and 5, the abnormal measurement indicators of the proposed algorithm are more prominent than those of the OLAP approach during the event period.

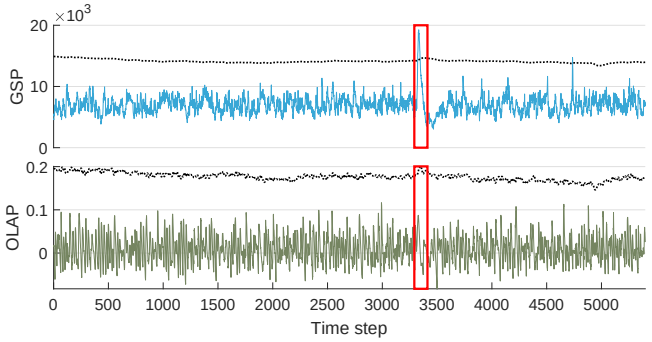

Fig. 6: Abnormal event indicators of the GSP based approach and the OLAP algorithm for the sample frequency event.

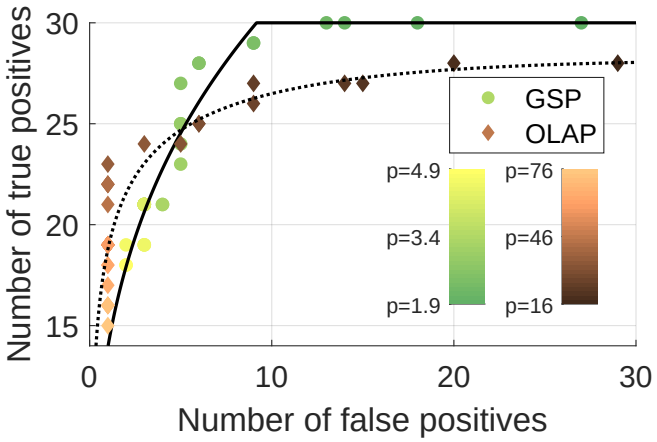

Fig. 7: Numbers of true positives and false positives with different values of p on the 30-event dataset.

Fig. 6 shows the abnormal event indicators derived from the proposed GSP-based approach and the OLAP algorithm for the sample generator tripping event. The dotted lines show the adaptive thresholds with $p = 2.2$ for GSP and $p = 18$ for OLAP, respectively. The peak of the abnormal event indicator of our proposed method falls in the event period while the OLAP algorithm fails to detect it. It's worth noting the proposed approach also produces a false positive between time step 4,500 and 5,000. We test both algorithms on all 30 events in our dataset. Fig. 7 shows the numbers of true positives and false positives with different values of p. Table II shows the F1 scores with $p = 2.5$ for GSP and $p = 36$ for OLAP, where they achieve the highest values for all test events. It is observed that the GSP based approach generally outperforms the OLAP algorithm on the dataset in terms of both precision and F1 score.

C. Execution Speed and Scalability of the Proposed Algorithm

In this subsection, we evaluate the scalability of the proposed GSP-based approach. For 30 power system events tested in the previous subsection, the average runtime of the proposed method on the 3-minute testing data is 6.16 seconds per event, which is shorter than the 132.88 seconds runtime of the OLAP algorithm. The enhanced execution speed is because most of the computation is carried out offline in our proposed algorithm. Note that the graph Laplacian does not need to be updated frequently in online abnormal event detection process.

TABLE II: F1 scores of the proposed GSP based approach and the OLAP algorithm

Method	GSP	OLAP
Category 1	0.7692	0.9
Category 2	1	0.8889
Category 3	0.8889	0.75
All Events	0.8750	0.8519

TABLE III: Scalability test results

Number of PMUs	30	60	90	120
Runtime	3.01 s	4.45 s	5.80 s	6.95 s

To validate the scalability of the proposed GSP-based event detection algorithm, we vary the number of PMUs for testing datasets in the range of 30 and 120 and record the runtime. The algorithm runtime and the corresponding number of PMUs are shown in Table III. By comparing the second and the fifth columns, we can see that the runtime of the algorithm only increases by a factor of 1.83 while the number of PMUs quadruples. These results show that the GSP based approach has excellent scalability.

IV. Conclusion

This paper develops a novel online event detection algorithm based on graph signal processing using steaming synchrophasor data. The proposed algorithm has two components: off-line training and online event detection. In the off-line training stage, we propose a graph Laplacian construction algorithm, which separately captures the spatial and temporal correlation structures of streaming synchrophasor data. In the online event detection stage, abnormal measurement and event indicators are derived based on the non-DC components of the graph Fourier transform of the PMU data. The testing results on real-world synchrophasor data in the U.S. show that our proposed algorithm outperforms the state-of-the-art benchmark algorithm in terms of both precision and execution speed. Furthermore, our proposed algorithm demonstrates excellent scalability.

Acknowledgment

This material is based upon work supported by the Department of Energy under Award Number DE-OE0000916.

References

[1] D.-I. Kim, T. Y. Chun, S.-H. Yoon, G. Lee, and Y.-J. Shin, "Wavelet-based event detection method using PMU data," *IEEE Transactions on Smart Grid*, vol. 8, no. 3, pp. 1154–1162, Oct. 2015.

[2] S. S. Negi, N. Kishor, K. Uhlen, and R. Negi, "Event detection and its signal characterization in PMU data stream," *IEEE Transactions on Industrial Informatics*, vol. 13, no. 6, pp. 3108–3118, Jul. 2017.

[3] S.-W. Sohn, A. J. Allen, S. Kulkarni, W. M. Grady, and S. Santoso, "Event detection method for the PMUs synchrophasor data," in *2012 IEEE Power Electronics and Machines in Wind Applications*, Jul. 2012, pp. 1–7.

[4] Y. Zhou, R. Arghandeh, H. Zou, and C. J. Spanos, "Nonparametric event detection in multiple time series for power distribution networks," *IEEE Transactions on Industrial Electronics*, vol. 66, no. 2, pp. 1619–1628, Jun. 2018.

[5] C. Hannon, D. Deka, D. Jin, M. Vuffray, and A. Y. Lokhov, "Real-time anomaly detection and classification in streaming PMU data," *arXiv preprint arXiv:1911.06316*, 2019.

[6] L. Xie, Y. Chen, and P. Kumar, "Dimensionality reduction of synchrophasor data for early event detection: Linearized analysis," *IEEE Transactions on Power Systems*, vol. 29, no. 6, pp. 2784–2794, Nov. 2014.

[7] J. Wu, J. Xiong, P. Shil, and Y. Shi, "Real time anomaly detection in wide area monitoring of smart grids," in *2014 IEEE/ACM International Conference on Computer-Aided Design (ICCAD)*, Nov. 2014, pp. 197–204.

[8] Z. Ling, R. C. Qiu, X. He, and L. Chu, "A new approach of exploiting self-adjoint matrix polynomials of large random matrices for anomaly detection and fault location," *IEEE Transactions on Big Data*, May 2019.

[9] X. Shi and R. Qiu, "Dimensionality increment of PMU data for anomaly detection in low observability power systems," *arXiv preprint arXiv:1910.08696*, 2019.

[10] P. Gao, M. Wang, S. G. Ghiocel, J. H. Chow, B. Fardanesh, and G. Stefopoulos, "Missing data recovery by exploiting low-dimensionality in power system synchrophasor measurements," *IEEE Transactions on Power Systems*, vol. 31, no. 2, pp. 1006–1013, Apr. 2015.

[11] Y. Hao, M. Wang, J. H. Chow, E. Farantatos, and M. Patel, "Modelless data quality improvement of streaming synchrophasor measurements by exploiting the low-rank Hankel structure," *IEEE Transactions on Power Systems*, vol. 33, no. 6, pp. 6966–6977, Jun. 2018.

[12] J. Shi, N. Yu, E. Keogh, H. K. Chen, and K. Yamashita, "Discovering and labeling power system events in synchrophasor data with matrix profile," in *2019 IEEE Sustainable Power and Energy Conference (iSPEC)*. IEEE, Nov. 2019, pp. 1827–1832.

[13] A. Neumaier and T. Schneider, "Estimation of parameters and eigenmodes of multivariate autoregressive models," *ACM Transactions on Mathematical Software (TOMS)*, vol. 27, no. 1, pp. 27–57, Mar. 2001.

[14] G. Schwarz *et al.*, "Estimating the dimension of a model," *The annals of statistics*, vol. 6, no. 2, pp. 461–464, 1978.

[15] A. Sandryhaila and J. M. Moura, "Big data analysis with signal processing on graphs," *IEEE Signal Processing Magazine*, vol. 31, no. 5, pp. 80–90, 2014.

[16] L. Stanković and E. Sejdić, *Vertex-Frequency Analysis of Graph Signals*. Springer, 2019.

[17] A. Sandryhaila and J. M. Moura, "Discrete signal processing on graphs," *IEEE Transactions on Signal Processing*, vol. 61, no. 7, pp. 1644–1656, Jan. 2013.